

MONASH UNIVERSITY

Department of Mechanical Engineering

ENGINEERING PRACTICES 3423

Authentic Design Project

FINAL REPORT

# AUSROC II

"Design of a Bi-Propellant Liquid Fuelled Rocket"

Project Engineers

Mark Blair (Mech. Eng.)  
Peter Kantzos (Mech. Eng.)  
Dominic Marinelli (Elec. Eng.)

## ACKNOWLEDGEMENTS

The success of this project can be attributed to the support and sponsorship given by a great number of persons and companies. Without this support and sponsorship, AUSROC II would never have proceeded past the drawing board. We would very much like to thank the following persons, companies and institutions for their assistance and commitment towards the development, construction and test flight of AUSROC II:

J. Stecki, Monash University (Mech. Eng.)

J. Matthew, Monash University (Mech. Eng.)

W. Melbourne, Monash University (Mech. Eng.)

M. Wadsley, Monash University (Chem. Eng.)

N. Murray, Monash University (Civil Eng.)

Monash University Mechanical Engineering Labs.

N. Liedinger, BHP Melbourne Research Labs

Pacific Rocket Society (U.S.A.)

Aeronautical Research Labs

Aerospace Technologies of Aust.

Bestobell Engineering Products

B.H.P.

Brathstray Ltd.

Brown & Dureau International

BTR Indeng

C.I.G.

Comalco

Davidson Pty. Ltd.

D.S.T.O. Range Measurements Branch S.A.

Hawker De Havilland

H.I. Fraser

Mobil

NEC

Philips

R.A.A.F.

## NOMENCLATURE

A = Chamber surface area ( $m^2$ )  
Ae = Nozzle exit area ( $m^2$ )  
Ai = Injection hole area ( $m^2$ )  
Am = Coolant mean passage area ( $m^2$ )  
Ap = Coolant passage area ( $m^2$ )  
At = Nozzle throat area ( $m^2$ )  
Cd = Drag/Discharge coefficient  
Cf = Thrust coefficient  
Cp = Specific heat, constant pressure (J/mol K)  
Cv = Specific heat, constant volume (J/mol K)  
D = Hydraulic diameter (m)  
E = Modulus of elasticity (MPa)  
F = Thrust (N)  
f = Friction factor  
G = Gibbs free energy (J/kg)  
g = 9.81 = Acceleration due to gravity ( $m/s^2$ )  
H = Enthalpy (J/kg)  
h = Heat transfer coefficient ( $W/m^2 K$ )  
ha = Atmospheric coefficient ( $W/m^2 K$ )  
hg = Combustion gas coefficient ( $W/m^2 K$ )  
hl = Coolant liquid coefficient ( $W/m^2 K$ )  
Isp = Specific Impulse (sec)  
k = Specific heat ratio (Cp/Cv)  
K = Thermal conductivity (W/m K)  
L = Length (m)  
L\* = Characteristic chamber length (m)  
m = Mass (kg)  
mf = Mass flow rate of fuel (kg/s)  
mox = Mass flow rate of oxidizer (kg/s)  
Mr = Molecular weight (g/mol)  
n = Number of Mol  
P = Pressure (Pa)  
P1 = Combustion pressure (Pa)  
P2 = Nozzle exit pressure (Pa)  
P3 = Atmospheric pressure (Pa)  
P = Pressure drop through coolant passage (Pa)  
Pt = Nozzle throat pressure (Pa)  
Pw = Wetted Perimeter (m)  
q = Heat flux ( $W/sq.m$ )  
Q = Volumetric flowrate ( $m^3/s$ )  
r = Radius (m)  
Re = Reynolds number  
R = 8.3142 = Gas constant  
S = Entropy (J/mol K)  
s = Stress (MPa)  
t = Wall thickness (m)

$T$  = Temperature (K)  
 $T_a$  = Ambient temperature (K)  
 $T_c$  = Combustion temperature (K)  
 $T_g$  = Combustion gas temperature (K)  
 $T_{in}$  = Coolant inlet temperature (K)  
 $T_l$  = Liquid coolant temperature (K)  
 $T$  = Coolant exit temperature (K)  
 $T_{sa}$  = Outer wall temp on outside (K)  
 $T_{sl}$  = Outer wall temp on inside (K)  
 $T_{wg}$  = Chamber wall temp on gas side (K)  
 $T_{wl}$  = Chamber wall temp on coolant side (K)  
 $v$  = Corrected exhaust velocity (m/s)  
 $v_1$  = Combustion chamber gas velocity (m/s)  
 $v_2$  = Nozzle exit velocity (m/s)  
 $v_t$  = Nozzle throat velocity (m/s)  
 $V_c$  = Combustion chamber volume ( $m^3$ )  
 $V_f$  = Volume flow rate of fuel ( $m^3/s$ )  
 $V_{ox}$  = Volume flow rate of oxidizer ( $m^3/s$ )

$\alpha$  = Nozzle expansion half angle (degrees)  
 $\zeta_t$  = Thrust correction factor  
 $\lambda$  = Nozzle angle correction factor  
 $\gamma$  = Relative roughness (m)  
 $\nu$  = Kinematic viscosity ( $m^2/s$ )  
 $\nu$  = Poisson's ratio  
 $\rho$  = Density ( $kg/m^3$ )

# CONTENTS

<b>ACKNOWLEDGEMENTS</b>	<b>I</b>
<b>PREFACE</b>	<b>III</b>
<b>NOMENCLATURE</b>	<b>IV</b>
<b>CONTENTS</b>	<b>VI</b>
 <b>CHAPTER 1: INTRODUCTION</b>	
<b>1.1 Objectives</b>	<b>1</b>
<b>1.2 Basic Concepts of Rocketry</b>	<b>1</b>
<b>1.2.1 Combustion Chambers</b>	<b>1</b>
<b>1.2.2 Pressure Feed Systems</b>	<b>2</b>
<b>1.2.3 Turbopump Feed Systems</b>	<b>2</b>
<b>1.2.4 Vehicle Guidance</b>	<b>2</b>
<b>1.2.5 Telemetry Systems</b>	<b>3</b>
 <b>CHAPTER 2: THERMOCHEMICAL PROPELLANT ANALYSIS</b>	
<b>2.1 Propellant Selection</b>	<b>9</b>
<b>2.2 Thermochemical Reaction Calculations</b>	<b>17</b>
 <b>CHAPTER 3: COMBUSTION CHAMBER DESIGN</b>	
<b>3.1 Determination of Chamber Configuration</b>	<b>41</b>
<b>3.2 Heat Transfer Analysis</b>	<b>48</b>
<b>3.3 Hydraulic Losses in Cooling Passage</b>	<b>53</b>
<b>3.5 Chamber Material and Stress Analysis</b>	<b>55</b>
<b>3.6 Engine Thrust Mount</b>	<b>62</b>

## **CHAPTER 4: INJECTOR DESIGN**

- 4.1 Injector Design Calculations 64**
- 4.2 Injector Material and Geometry 70**

## **CHAPTER 5: DESIGN OF PROPELLANT STORAGE TANKS**

- 5.1 Determination of Tank Configuration 74**
- 5.2 Tank Material Selection and Stress Analysis 77**

## **CHAPTER 6: DESIGN OF PRESSURE FEED SYSTEM**

- 6.1 Pressure Feed Requirements 81**
- 6.2 Component Selection for Feed System 83**

## **CHAPTER 7: PAYLOAD AND RECOVERY MODULES**

- 7.1 Payload Facilities 86**
- 7.2 Recovery System 87**

## **CHAPTER 8: LAUNCH INFRASTRUCTURE**

- 8.1 Launch Rack Requirements 92**
- 8.2 Rocket Launch Lugs 93**
- 8.3 Static Test Facilities 93**
- 8.4 Launch Rack Configuration 93**

## **CHAPTER 9: VEHICLE CONSTRUCTION AND TESTING**

## **CHAPTER 10: AERODYNAMIC ANALYSIS**

## **CHAPTER 11: LAUNCH SEQUENCE INSTRUCTIONS**

**CHAPTER 12: LAUNCH DAY**

**CHAPTER 13: POST FLIGHT ANALYSIS**

<b>BIBLIOGRAPHY</b>	<b>102</b>
<b>APPENDIX A: THERMOCHEMICAL ANALYSIS RESULTS</b>	<b>104</b>
<b>APPENDIX B: CHEMIX PROGRAM LISTINGS</b>	<b>133</b>
<b>APPENDIX C: CHAMBER EQUATION DERIVATIONS</b>	<b>139</b>
<b>APPENDIX D: REGULATOR, VALVE &amp; ACTUATOR DATA</b>	<b>146</b>
<b>APPENDIX E: CORRESPONDENCE OUT</b>	<b>174</b>
<b>APPENDIX F: CORRESPONDENCE RECIEVED</b>	<b>200</b>
<b>APPENDIX G: PARACHUTE CANOPY DATA</b>	<b>216</b>



# CHAPTER 1

## INTRODUCTION

### 1.1 OBJECTIVES

"It is the objective of this project to undertake a complete design study for a bi-propellant liquid fuelled rocket which can be built by amateurs at a reasonable cost. It is also envisaged that a testable prototype could be constructed pending financial availability".

It is intended that this project will give a large amount of engineering experience to the participating students. This is due to the large number of engineering disciplines that are required in the design of a rocket system.

The primary objectives relating to the above statement are listed as follows:

<b>Minimum Altitude Gain</b>	<b>30 km</b>
<b>Minimum Velocity Gain</b>	<b>700 m/s</b>
<b>Thrust Level</b>	<b>1000 kg (9810 N)</b>

### 1.2 BASIC CONCEPTS OF ROCKETRY

Many systems go together to make up a rocket and they all must be compatible for successful operation. Below is an outline of some of the basic concepts of liquid fuelled rockets.

#### 1.2.1 COMBUSTION CHAMBERS

A combustion chamber is essentially a special combustion device where liquid propellants are metered, injected, atomized, mixed, and burned at a high combustion pressure to form gaseous reaction products, which in turn are accelerated and ejected at high velocities. Due to the high rate of energy given off, the cooling, stability of combustion, ignition, and injection problems deserve special consideration. Since combustion chambers are airborne devices, the weight has to be a minimum. A desirable combustion chamber therefore, combines lightweight construction with high performance, simplicity and reliability. The combustion chamber must be protected from the high rates of heat transferred to the chamber walls. There are at least 3 accepted ways of cooling the walls of a thrust chamber with liquid propellant: regenerative cooling, film cooling and transpiration or sweat cooling and each will be discussed in more detail in later chapters. Fig.1.1 shows a basic combustion chamber and the associated nomenclature that will be used throughout this report.

### **1.2.2 PRESSURE FEED SYSTEMS**

In these systems a high pressure gas is used to expel the propellants from the storage tanks into the combustion chamber. This is the simplest method and the cheapest. It is used primarily in low thrust engines and small rockets due to its simplicity but in large rockets, the weight of the pressurized propellant tanks becomes prohibitive and greatly decreases the effectiveness of the rocket unit. Pressure feed systems consist of 2 pressure vessel propellant tanks which are maintained at the feed pressure by a pressurizing gas which is fed from a high pressure bottle via regulators to the propellant tanks. Other items required include: valves, actuators, solenoids, relief valves, etc. Fig.1.2 shows a simplified pressure feed system and labels the system components.

### **1.2.3 TURBOPUMP FEED SYSTEMS**

The turbopump rocket system pressurizes the propellants by means of pumps, which in turn, are driven by turbines. The turbines derive their power from the expansion of hot gases. A separate gas generator ordinarily produces these gases in the required quantities and at the desired turbine inlet temperature by means of a chemical reaction similar to the reaction in the combustion chamber. Turbopump rocket systems are usually used on high thrust and long duration rocket units; they are usually lighter than other types of feed systems for these applications. Their weight is essentially independent of thrust duration. In these systems the propellant tanks need not hold any high pressures and thus the tanks generally have a light weight construction. Fig.1.3 shows a simplified turbopump feed system and labels the system components.

### **1.2.4 VEHICLE GUIDANCE**

Aerodynamic stability of vehicles is a prerequisite to flight. This stability can be built in by proper design so that the flying vehicle will be inherently stable. By placing fixed fins at the rear of the rocket, the centre of pressure can be moved such that it is located behind the centre of gravity, thus ensuring natural stability. Stability can also be obtained by appropriate controls, such as the aerodynamic control surfaces on an airplane or jet vanes immersed in the exhaust gas of a rocket on a guided missile. For this active control to be effective the centre of pressure should coincide with the centre of gravity (ie neutral stability) such that the forces required to steer the vehicle will be a minimum. In the case of non-active guidance, the first few seconds of flight are its least stable due to the fact that it is travelling slowest at this stage. In these cases a launch rail is generally used to guide the vehicle during this critical period. Fig.1.4 illustrates several types of guidance.

### **1.2.5 TELEMETRY SYSTEMS**

In the test flight or normal operation of a rocket there are usually many parameters that require monitoring. These include: accelerations, velocities, pressures, temperatures, stresses, experiments, propellant flows etc. To get this information various sensors must be incorporated into the vehicle. The data from the sensors must be either stored onboard the rocket or transmitted back to a receiving ground station. The later is the most common method and requires that the rocket carry a transmitter and power supply to send the data back to ground. Thus an antenna must be incorporated into the airframe as well. Fig.1.5 shows a block diagram representing the elements of a telemetry system.

# CHAPTER 2

## THERMOCHEMICAL PROPELLANT ANALYSIS

### 2.1 PROPELLANT SELECTION

The propellants, which are the working substance of rockets, constitute the fluid which undergoes chemical and thermodynamic changes. There are a large variety of liquid propellant combinations which have been analytically and experimentally investigated. Unfortunately, it has not been possible to discover an ideal liquid propellant combination which will have only desirable characteristics. Almost every liquid propellant, especially every liquid oxidizing agent, has at least one or more undesirable properties, and no standard liquid propellant has yet been developed.

A monopropellant contains an oxidizing agent and combustible matter in a single substance. It may be a mixture of several compounds, or it may be a homogeneous chemical agent.

A bipropellant rocket has two separate propellants which are mixed inside the combustion chamber. The majority of successful liquid propellant rockets have used bi-propellants. Occasionally rockets with three or more liquid propellants have been used, but never very extensively.

Due to the fact that no single propellant has all desirable properties, the selection of the propellant combination is a compromise of many parameters as listed below:

**Economic:**

- availability in large quantities
- low cost
- logistics of production
- simplicity of production process

**Performance of Propellants:**

- specific impulse
- effective exhaust velocity
- specific propellant consumption
- high energy content
- low molecular mass

**Common Physical Hazards:**

- corrosive effects
- explosive hazards
- fire hazards
- toxicity

- Desirable Physical Properties:**
- low freezing point
  - high specific gravity
  - chemical stability
  - high specific heat
  - high thermal conductivity
  - high boiling point
  - low viscosity
  - low vapour pressure

Propellants can be classified into two groups according to the type of ignition used. The first group is termed 'HYPERGOLIC' due to the fact that these combinations ignite spontaneously upon contact with each other. Nonspontaneously ignitable propellants have to be heated by external means before ignition can begin. Table 2.1 shows many different types of propellants that can be used for rocket propulsion.

Many propellants are listed in table 2.1 but only a few of these are commonly used. The more common propellants are described in more detail below:

## **LIQUID OXIDIZERS**

**Liquid Oxygen:** Chemical Formula - O<sub>2</sub>  
Boiling point - 90 K  
Specific gravity - 1.14

Liquid oxygen is currently used in conjunction with alcohols, jet fuels (kerosene types), gasoline and hydrogen. It burns with a bright white-yellow flame with most hydrocarbons and usually does not burn spontaneously. It is a noncorrosive and nontoxic liquid. Because liquid oxygen evaporates rapidly, it cannot be stored readily for any great length of time. It is necessary to insulate all lines, tanks, valves, etc.

**Liquid Fluorine:** Chemical Formula - F<sub>2</sub>  
Boiling point - 54 K  
Specific gravity - 1.5

In combination with most fuels, liquid fluorine affords higher values of performance and energy than other oxidizers. It is extremely toxic, corrosive and reactive. Special passivation techniques and insulation have to be used on containers, pipelines and valves to permit handling of liquid fluorine in common construction metals. The production of liquid fluorine is an expensive process and commercial consumption is low.

**Nitric Acid:** Chemical Formula - HNO<sub>3</sub>  
Boiling point - 411 K  
Specific gravity - 1.5

Red fuming nitric acid is the most common type, consisting of concentrated nitric acid and between 5-20% nitrogen dioxide. It is corrosive, toxic and requires special handling precautions. Nitric acid affords a lower specific impulse than most other oxidizers.

**Nitrogen Tetroxide:**            Chemical Formula -  $N_2O_4$   
Boiling point   - 294 K  
Specific gravity - 1.44

Nitrogen Tetroxide is the most common storable oxidizer used today but its liquid temperature range is narrow and it is easily frozen or vapourized. It is hypergolic with many fuels. It is toxic and has a high vapour pressure, necessitating heavy tanks.

## **LIQUID FUELS**

**Hydrocarbon Fuels:**            Chemical Formula -  $C_xH_y$   
Boiling point   - varies  
Specific gravity - varies

These include gasoline, kerosene, diesel oil and turbojet fuel. Their physical properties and chemical composition vary widely. They are relatively easy to handle, and there is an ample supply of these fuels at low cost. Table 2.2 shows the properties of several hydrocarbon fuels.

**Table 2.2:** Properties of Hydrocarbon Fuels

**Liquid Hydrogen:** Chemical Formula -  $H_2$   
Boiling point - 20 K  
Specific gravity - 0.07

Liquid hydrogen gives high performance when burned with liquid oxygen or liquid fluorine and is an excellent regenerative coolant. Of all known fuels it is the lightest and the coldest. Special insulation provision must be used and care taken to select materials for the storage tanks.

**Hydrazine:** Chemical Formula -  $N_2H_4$   
Boiling point - 386 K  
Specific gravity - 1.01

Hydrazine is a toxic and colorless liquid. It is spontaneously ignitable with nitric acid and nitrogen tetroxide. It is an excellent monopropellant when decomposed by a suitable catalyst. It generally gives good performance when compared with many common fuels.

**Unsymmetric Dimethylhydrazine:** Chemical Formula -  $(CH_3)_2NNH_2$   
Boiling point - 336 K  
Specific gravity - 0.61

This is a more stable derivative of hydrazine. It gives slightly lower performance than pure hydrazine and is usually used in a mixture with hydrazine itself.

**Monomethylhydrazine:** Chemical Formula -  $CH_3NHNH_2$   
Boiling point - 361 K  
Specific gravity - 0.88

This is another derivative of hydrazine. It has better shock resistance to blast waves, better heat transfer properties and a better liquid temperature range than pure hydrazine.

**Table 2.3** shows the chemical properties of some of the most common liquid propellants.

The selection of our propellant combination was based on 4 considerations: cost, availability, performance and ease of handling and storage.

Liquid fluorine gives the highest performance but was eliminated due to difficulties involved in handling and lack of availability. Nitric acid is a good storable oxidizer and is readily available at low cost but it was eliminated due to its relatively low performance when compared to other oxidisers. Nitrogen tetroxide is a storable high performance oxidizer but it is not readily available in the required concentrations or quantities that we require. Liquid Oxygen is readily available in large quantities from air liquification plants at very low costs (approximately 50c/Lt) and gives high

performance with various fuels. While liquid oxygen presents some storage problems due to its cryogenic nature, its other properties make it the most favourable oxidizer for this particular project.

With liquid oxygen chosen as the oxidizer, we can eliminate Hydrazine fuel and its derivatives due to their lower performance with liquid oxygen and also due to their low availability in high concentrations. Liquid hydrogen gives a higher performance with liquid oxygen than any other fuel. However, liquid hydrogen has a very low density and requires large and hence heavy propellant storage tanks. It boils at around 20 K and requires very special materials to prevent hydrogen embrittlement and special insulation to prevent boil-off during storage. Liquid hydrogen has a low to nil availability in this country and was eliminated for these reasons. Alcohols are readily available at low cost, are storable and non toxic but afford lower performance than the hydrocarbon fuels and thus were eliminated. Hydrocarbon fuels give good performance in combination with liquid oxygen. They are storable, quite easy to handle and available in large quantities at low cost. Kerosene type hydrocarbons are most commonly used as rocket fuels so we chose to use readily available JA-1 Jet fuel, which is a kerosene derivative, as the fuel for this project.

The LOX/Kero propellant combination is not a hypergolic mixture so an ignition system will be required to ignite the propellant at startup and from then on the combustion will be self sustaining provided that instabilities and other phenomenon do not extinguish the flame or force it outside the chamber. **Table 2.4** shows the chemical properties of liquid oxygen (now on referred to as LOX) and JA-1 Jet fuel as obtained from the Mobil Oil company.

**TABLE 2.4**  
CHEMICAL PROPERTIES OF LIQUID OXYGEN AND JA-1 JET FUEL

Property	Liquid Oxygen	JA-1 Jet Fuel
Chemical Formula	O <sub>2</sub>	C <sub>7.135</sub> H <sub>14.187</sub>
Molecular Mass	32	175 (av.)
Melting Point (K)	54.36	226
Boiling Point (K)	90.19	477-561 (1atm.)
Density (kg/cu.m)	1141.1 (at b.p.)	800 (at 298 K) 600 (at 400 K)
Specific Heat (J/kgK)	1738.14 (sat.liq.)	2090 (273-373 K)
H <sub>v</sub> (kJ/kg)	218.2	246
H <sub>c</sub> (MJ/kg)		42.8 (s.t.p.)
Conductivity (W/mK)	0.150	0.16 (273 K) 0.12 (373 K)
Viscosity (Centipoise)	0.87 (54 K) 0.19 (90 K)	0.75 (290 K) 0.21 (366 K)
Availability	Good	Good
Storability	Poor	Good
Toxicity	Low	Low
Corrosiveness	Low	Low



## 2.2 THERMOCHEMICAL REACTION CALCULATIONS

To analyse the performance of a particular propellant combination we have to first calculate the combustion chamber gas conditions and the conditions of the exhaust products. These conditions include:

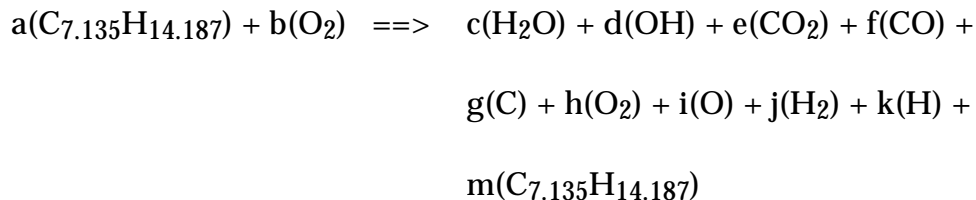
- combustion and exhaust temperature
- average molecular weight of products
- specific heat ( $C_p$ )
- enthalpy changes
- entropy

These can be determined, through iteration procedures, from the chemical composition of the initial propellant mixture, the prereaction temperatures of the propellants and the predetermined combustion chamber pressure. For the Lox/Kerosene mixture that we are using, we have 10 possible species that can exist in the combustion process since dissociation readily occurs at high temperatures. There may be more species but the concentrations would be very low and have no direct effect on the result.

These are:

- Kerosene[JA-1](carbon/hydrogen ratio  $C_{7.135}H_{14.187}$ )
- Oxygen ( $O_2$ )
- Oxygen (O)
- Hydrogen ( $H_2$ )
- Hydrogen (H)
- Carbon Dioxide ( $CO_2$ )
- Carbon Monoxide (CO)
- Carbon (C)
- Hydroxide (OH)
- Water ( $H_2O$ )

The general form of the reaction equation can be shown as:



Where:  $7.135a = 2e + f + g + 7.135m$  [for carbon]

$14.187a = 2c + d + 2j + k + 14.187m$  [for hydrogen]

$2b = c + d + 2e + f + 2h + i$  [for oxygen]

(Note: a,b,c,d,e,f,g,h,i,j,k,m are all mol ratios )

The analysis of the heat balance requires knowledge of the values of the specific heat ( $C_p$ ), the enthalpy ( $H$ ), the entropy ( $S$ ) and the Gibbs free energy ( $G$ ) for each of the species as a function of the absolute temperature. Other data such as the heat of melting and vapourization can be included wherever needed. The Gibbs free energy ( $G$ ), or chemical potential, is a derived function or property of the state of a chemical material describing its thermodynamic potential and is defined as:

$$\begin{aligned}G &= U + PV - TS = H - TS \\H &= C_p \times dT \\S &= H / T\end{aligned}$$

where:  $U$ =internal energy  
 $P$ =pressure  
 $V$ =volume  
 $H$ =enthalpy  
 $T$ =temperature (abs.)  
 $S$ =entropy

Where there is more than 1 species in the product, the Gibbs free energy is given by:

$$G = \sum ( G_i \times n_i ) \quad \begin{array}{l} i=1 \text{ to } \# \text{ species} \\ n_i=\text{mol fraction} \end{array}$$

Equilibrium mol ratios, combustion temperatures and heat balances of a particular propellant combination at a particular combustion pressure can be found through the process of minimization of Gibbs free energy. When a system is at its lowest energy level it is in its most stable position, ie equilibrium. Since several of the terms in the Gibbs free energy equation are functions of temperature, an iterative method must be used to converge on a solution. We performed iterative calculations on 9 different propellant mass ratios (Mass Oxidizer/Mass Fuel) using the following software package:

CSIRO THERMOCHEMISTRY SYSTEM VSN 5.1M IBM-PC  
PROGRAM CHEMIX

COPYRIGHT 1988,89 - CSIRO Div. MINERAL PRODUCTS  
MONASH UNIVERSITY  
MICHAEL W. WADSLEY

Before the calculations were performed, the following assumptions were made:

1. The working substance is homogeneous and invariant in composition throughout the combustion chamber.
2. The working substance obeys the perfect gas laws.
3. There is no friction.
4. There is no heat transferred (lost) across the chamber walls; the combustion is thus Adiabatic.
5. The flow is constant and in steady state

6. There is no shock, vibration or discontinuities.
7. Equilibrium is achieved in the combustion process
8. The velocity, pressure, temperature and density are uniform across any section normal to the chamber axis.

The gases entering the nozzle experience an Isentropic, reversible, one dimensional expansion process which is accompanied by a drop in temperature and pressure and a conversion of thermal energy into kinetic energy. The state of the gas at all times within the expansion process is fixed by the entropy of the system which remains constant.

The expansion process can be treated in 2 different ways:

1. Assuming infinitely slow reaction rate. The composition of the products is invariant throughout the nozzle, ie no reaction takes place as the temperature and pressure drop along the nozzle axis. In this case the composition of the exhaust product is identical to that of the combustion product. This situation is referred to as FROZEN EQUILIBRIUM.

2. Assuming infinitely fast reaction rate. Instantaneous chemical equilibrium among all species is maintained under the continuously variable temperature and pressure along the nozzle axis. The product composition will thus vary along the length of the nozzle. This is commonly referred to as SHIFTING EQUILIBRIUM. In this process extra energy is released due to the recombination of free radicals and atomic species which become unstable at the lower temperatures reached in the expansion process. This leads to higher performance values being obtained for shifting equilibrium than for frozen equilibrium.

There were 3 sets of calculations performed on each propellant mass ratio:

1. Adiabatic Combustion of Kerosene
2. Isentropic Shifting Equilibrium Expansion of Products.
3. Isentropic Frozen Equilibrium Expansion of Products.

We set the combustion pressure to 2MPa (19.738 atm). Higher combustion pressures lead to higher performance values but since we chose to use a pressure feed system for the propellant delivery, a higher combustion pressure would have led to heavier propellant tank structures due to the increased pressure needed for the propellant delivery. The exit or exhaust pressure was set at 101325Pa (1 atm) as this would give an optimum expansion ratio at launch (sealevel).

**Appendix A** contains the results of the thermochemical analysis performed by the CHEMIX program on the propellant mass ratios: 1.6, 1.8, 2.0, 2.2, 2.3, 2.4, 2.6, 2.8, 3.0. **Appendix B** shows the 2 program listings used in the CHEMIX package to obtain the necessary results.

The results of the analysis are also shown in **table 2.6** and graphically, with each parameter plotted against propellant mass ratio, in the following figures:

- Fig.#**
- 2.1** Temperature
  - 2.2** Composition of Combustion Product
  - 2.3** Composition of Shifting Equilibrium Exhaust Product
  - 2.4** Molecular Weight of Products
  - 2.5** Enthalpy of Products
  - 2.6** Entropy of Products
  - 2.7** Specific Heats of Products
  - 2.8** Specific Heat Ratios of Products
  - 2.9**  $d(H)$  of Product Expansion
  - 2.10** Nozzle Exhaust Velocity
  - 2.11** Specific Impulse

We decided, for our calculations, to use the mass ratio which yielded the optimum specific impulse for frozen equilibrium.

$$\text{Propellant Mass Ratio} = 2.2 = (M_{ox}/M_f)$$

$$\text{Exhaust Velocity (ideal)} = 2450.3 \text{ m/s}$$

$$\text{Specific Impulse (ideal)} = 249.8 \text{ sec}$$

These ideal values must be multiplied by a correction factor which compensates for the non-ideal conditions present in a real rocket motor. We chose to use a velocity correction factor of 0.94 which is typical for rocket motors of this type. The new values are then:

$$\text{Exhaust Velocity (corrected)} = 2303.3 \text{ m/s}$$

$$\text{Specific Impulse (corrected)} = 234.8 \text{ sec}$$

**TABLE 2.6****Comparison of THERMOCHEMICAL data**

Mixture Ratio	Tc (°K)	Te (F) (°K)	Te (S) (°K)	Mr(av) (F exit)	Mr(av) (S exit)
1.6	2682.5	1410.2	1462.9	18.21	18.27
1.8	3020.1	1642.1	1768.6	19.43	19.68
2.0	3250.9	1808.6	2066.4	20.51	21.07
2.2	3391.7	1916.0	2345.7	21.42	22.41
2.3	3436.7	1952.2	2468.3	21.83	23.04
2.4	3469.3	1979.5	2572.3	22.21	23.63
2.6	3508.8	2015.6	2712.2	22.89	24.61
2.8	3526.4	2035.6	2778.8	23.49	25.38
3.0	3531.1	2045.4	2804.7	24.04	26.02

Note: (F) refers to a fixed equilibrium condition during the expansion process in the nozzle

(S) refers to a changing equilibrium condition during the expansion process in the nozzle

$Mr(av) = \text{mass}(g) / \text{mol}$

MIXTURE RATIO = Mass(Oxidizer) / Mass(Fuel)

COMBUSTION PRESSURE = 2,000,000 Pa

EXIT PRESSURE = 101,325 Pa

FUEL = Kerosene (JA-1 Jet Fuel)

OXIDIZER = Liquid Oxygen

**TABLE 2.6 (Continued)****[Comparison of THERMOCHEMICAL data]****CHAMBER HEAT CAPACITIES**

Mixture Ratio	C <sub>p</sub> (C) J/mol K	C <sub>v</sub> (C) J/mol K	k (C) J/mol K
1.6	36.19	27.88	1.298
1.8	37.86	29.55	1.283
2.0	39.16	30.84	1.270
2.2	40.10	31.78	1.262
2.3	40.46	32.14	1.259
2.4	40.77	32.46	1.256
2.6	41.24	32.93	1.253
2.8	41.58	33.27	1.250
3.0	41.87	33.55	1.248

**FROZEN EXIT HEAT CAPACITIES**

Mixture Ratio	Exit C <sub>p</sub> J/mol K	Exit C <sub>v</sub> J/mol K	Exit k J/mol K
1.6	33.22	24.90	1.334
1.8	34.73	26.42	1.315
2.0	35.99	27.67	1.300
2.2	36.92	28.61	1.291
2.3	37.29	28.98	1.287
2.4	37.60	29.28	1.284
2.6	38.10	29.77	1.279
2.8	38.44	30.13	1.276
3.0	38.71	30.40	1.273

Note: (C) denotes the combustion chamber conditions

$$C_p(\text{av}) = H(T-298) / (T-298)$$

$$C_v(\text{av}) = C_p - 8.3142$$

$$k(\text{av}) = C_p / C_v$$

FROZEN refers to a fixed equilibrium condition during the expansion process in the nozzle

**TABLE 2.6 (Continued)****[Comparison of THERMOCHEMICAL data]****SHIFTING EXIT HEAT CAPACITIES**

Mixture Ratio	Exit Cp J/mol K	Exit Cv J/mol K	Exit k J/mol K
1.6	33.74	25.43	1.327
1.8	35.66	27.35	1.304
2.0	37.67	29.36	1.283
2.2	39.66	31.35	1.265
2.3	40.60	32.29	1.258
2.4	41.43	33.12	1.251
2.6	42.67	34.36	1.242
2.8	43.43	35.12	1.237
3.0	43.89	35.58	1.234

**HEAT OUTPUTS**

Mixture Ratio	H <sub>C</sub> H(T-298) J/mol	Entropy S J/mol K	Hexit (F) J/mol	Hexit (S) J/mol
1.6	86,302.5	234.24	36,943	39,304
1.8	103,046.5	245.86	46,687	52,446
2.0	115,625.4	254.76	54,363	66,615
2.2	124,036.1	261.23	59,743	81,218
2.3	126,977.5	263.78	61,681	88,115
2.4	129,294.6	266.02	63,218	94,232
2.6	132,415.8	269.46	65,410	103,014
2.8	134,246.0	272.05	66,799	107,749
3.0	135,360.6	274.21	67,652	110,124

Note: (C) denotes the combustion chamber conditions

$$C_p(\text{av}) = H(\text{T}-298) / (\text{T}-298)$$

$$C_v(\text{av}) = C_p - 8.3142$$

$$k(\text{av}) = C_p / C_v$$

(F) refers to a fixed equilibrium condition during the expansion process in the nozzle

(S) refers to a changing equilibrium condition during the expansion process in the nozzle

**TABLE 2.6 (Continued)****[Comparison of THERMOCHEMICAL data]****SHIFTING PERFORMANCE**

Mixture Ratio	d(H) Expansion J/kg	Exhaust Velocity m/s	I <sub>sp</sub> sec
1.6	2,755,000	2347.3	239.3
1.8	3,000,000	2449.5	249.7
2.0	3,161,000	2514.4	256.3
2.2	3,244,375	2547.3	259.7
2.3	3,260,909	2553.8	260.3
2.4	3,262,941	2554.6	260.4
2.6	3,233,888	2543.2	259.2
2.8	3,182,105	2522.7	257.2
3.0	3,122,250	2498.9	254.7

**FROZEN PERFORMANCE**

Mixture Ratio	d(H) Expansion J/kg	Exhaust Velocity m/s	I <sub>sp</sub> sec
1.6	2,720,769	2332.7	237.8
1.8	2,900,000	2408.3	245.5
2.0	2,987,000	2444.2	249.2
2.2	3,001,875	2450.3	249.8
2.3	2,992,121	2446.3	249.3
2.4	2,975,000	2439.3	248.7
2.6	2,927,778	2419.8	246.7
2.8	2,872,368	2396.8	244.3
3.0	2,816,000	2373.2	241.9

Note: FROZEN refers to a fixed equilibrium condition during the expansion process in the nozzle

SHIFTING refers to a changing equilibrium condition during the expansion process in the nozzle

EXHAUST VELOCITY =  $\sqrt{d(H)\text{expansion}}$

SPECIFIC IMPULSE = Exhaust Velocity / 9.81



## CHAPTER 3

### COMBUSTION CHAMBER DESIGN

#### 3.1 DETERMINATION OF CHAMBER CONFIGURATION

The geometry associated with a combustion chamber and the nozzle can be calculated using a series of equations derived from basic thermodynamic, pressure and force relations. (Derivations for some of the formulae, used in this chapter, are laid out in **Appendix C**).

The most critical dimension in the design of a combustion chamber is the nozzle throat. It is obtained using the following relation known as the **THRUST EQUATION**:

$$\mathbf{T} = \zeta_t \mathbf{C}_f \mathbf{P}_1 \mathbf{A}_t$$

**T** is defined as the Thrust force in Newtons that the combustion chamber is being designed to produce. For our rocket motor we specified a thrust rating of 9810 N (1000 kg).

$\zeta_t$  is the thrust correction factor. This parameter is introduced to relate an ideal combustion chamber to a real combustion chamber that involves losses within the system. These losses include incomplete combustion, heat lost through walls and frictional resistance. The actual thrust produced is lower than the thrust calculated for an ideal rocket and can be found using this empirical correction factor. Values of generally fall between 0.92 and 1.00. An accurate value for cannot be accurately determined until an engine firing is performed and measured data is obtained. For our calculations we chose to use a thrust correction factor of 0.96 which is mid-range between the 2 values shown above.

**P<sub>1</sub>** is the pressure at which the combustion proceeds. An increased combustion pressure leads to an increase in the chemical performance and also an increase in the combustion chamber weight. Combustion pressures, for liquid fuelled engines, generally range between 2-7 MPa (300-1000 psi). In a pressure feed rocket, which is what we are designing, an increase in combustion pressure would lead to an increase in the tank pressure and, thus, thicker and heavier tank walls. It is for this reason that we chose to use a combustion pressure of 2 MPa.

**A<sub>t</sub>** is the nozzle throat area and is usually the unknown variable in the thrust equation. It is determined to obtain the desired combustion pressure and thrust force for a particular combustion chamber.

**C<sub>f</sub>** is defined as the thrust coefficient and is derived in **appendix B**.

$$C_f = v [(2k^2/k-1)(2/k+1)^{(k+1/k-1)} (1 - (P_2/P_1)^{(k-1/k)})] + [(P_2-P_3)/P_1](A_e/A_t)$$

where:  $k = 1.262 =$  Ratio of Specific Heats  
 $P_1 = 2 \text{ MPa} =$  Combustion Pressure  
 $P_2 = 101325 \text{ Pa} =$  Exit Pressure  
 $P_3 = 101325 \text{ Pa} =$  Atmospheric Pressure

Since  $P_2=P_3$  the last term reduces to zero, thus:

$$C_f = 1.393$$

For any fixed pressure ratio ( $P_1/P_2$ ) the thrust coefficient has a maximum value when  $P_2=P_3$ . This value is called the '**Optimum Thrust Coefficient**'. It becomes apparent that as atmospheric pressure decreases, and all other parameters remain constant, the last term in the  $C_f$  equation tends to increase the value of  $C_f$  and thus of the thrust produced. This is commonly known as pressure thrust. **Fig. 3.1** shows the variation in pressure with altitude, while **Fig. 3.2** shows the variation in specific impulse with altitude.

From this we obtain:

$$A_t = 9810 / (0.96 \times 2000000 \times 1.393)$$

$$= 0.00367 \text{ m}^2$$

**Throat Diameter = 68.34 mm**

When the chamber is heated during the combustion process, the chamber wall expands thus enlarging the throat area and decreasing the thrust output. To compensate for this we decided to decrease the throat diameter to 68 mm.

**Throat Diameter = 68 mm**

Next, we calculated the nozzle exit area using the following relationship:

$$A_e = [ F T_c R (P_1/P_2)^{1/k} ] / [ v^2 P_1 M_r ]$$

Where:  $v = 2303.3 \text{ m/s} =$  corrected exhaust velocity  
 $T_c = 3391.7 \text{ K} =$  combustion temperature  
 $M_r = 21.42 =$  average molecular weight of products  
 $R = 8314.2$

Thus  $A_e = 0.01293 \text{ m}^2$   
**Exit diameter = 129 mm**

The next step involves determining the combustion chamber volume. Large chamber volumes lead to more efficient combustion, but also lead to heavier engines. It is therefore necessary to run a trade-off between size and combustion performance. Chamber volume is usually determined using semi empirical simplified relations determined from experimentation. The **Characteristic Chamber Length ( $L^*$ )** is defined as the length which a rocket motor of the same length would have if it were a straight tube and had no converging section.

$$L^* = V_c / A_t$$

Where:  $V_c = \text{Chamber volume (m}^3\text{)}$   
 $A_t = \text{Throat area (m}^2\text{)}$

Experimental results for a LOX/KERO propellant rocket motor give a Characteristic Chamber Length = 1m

Thus:  $V_c = 1 \times 0.00367 = 0.00367 \text{ m}^3$

The combustion chamber was to be manufactured from standard carbon steel pipe with I.D. = 154 mm (6"), therefore:

$$0.00367 = A_c \times L \quad \text{where: } L = \text{chamber length (m)}$$

$$L = 0.197 \text{ m}$$

To further enhance combustion efficiency, we extended the chamber length from 0.197m to .274m (top to throat) for geometric reasons.

$$L = 0.274 \text{ m}$$

There are 4 basic types of rocket nozzles; Conical nozzles, Bell or Contour nozzles, Plug nozzles and Expansion-Deflection nozzles as shown in Fig. 3.3. Of these, the conical nozzle is, by far, the easiest to manufacture but its performance is slightly less than that of the other 3 due to the exit angle leading to a non-axial component in the gas flow. This non-axial component increases with the nozzle exit angle. Small exit angles (2-5 degrees) lead to good performance but also to long and heavy nozzle expanders. We chose to use a conical nozzle and an expansion half angle  $\alpha=10.5$  degrees. This angle results in a nozzle angle thrust correction factor ( $\lambda$ ) given by:

$$\lambda = 0.5 (1 + \cos \alpha) \quad \text{where: } \alpha = \text{expansion half angle}$$

$$= 0.9916$$

This correction factor has been taken into account within the thrust correction factor ( $\zeta_t$ ) which was used in the **THRUST EQUATION** above.

The nozzle contraction half angle was set at 39 degrees. All these nozzle angles were connected by smooth and continuous radial transitions which allowed smooth flow conditions to exist throughout the nozzle and thus minimize losses. Fig. 3.4 shows the internal geometry of the combustion chamber.

## 3.2 HEAT TRANSFER ANALYSIS

In almost all designs and operations of rockets, considerable heat is transferred, and the phenomena of heat transmission often control the proper functioning of the units. Certain areas of heat transfer theory are considered in the field of rocketry.

These include:

- \* Heat transfer from the hot gases to the walls.
- \* Selection of propellants with favourable heat transfer characteristics.
- \* Exhaust flame heating of airframe and surrounding systems.
- \* Heat transfer, due to skin friction drag, to the flying vehicle at high speeds.

There are 3 accepted ways of cooling the walls of a thrust chamber with liquid propellant:

**1/ REGENERATIVE COOLING** requires the circulation of some or all of the propellant, fuel or oxidizer, through a jacket around the chamber.

**2/ FILM COOLING** requires the fuel or oxidizer liquid to be injected into the chamber to form a protective film of liquid or vapour adjacent to the walls.

**3/ TRANSPIRATION or SWEAT COOLING** requires a continuous injection of fluid over the entire surface of the wall, by using a porous wall material.

The heat transfer rate varies within the chamber and is usually highest at, and immediately upstream of, the nozzle throat. The lowest heat transfer rate is usually at the nozzle exit, since the exhaust gases have the lowest temperature at this point due to the isentropic expansion process. A typical heat transfer rate distribution is shown in **fig. 3.5**. Only 0.5 - 5 % of the total energy generated in the combustion process is transferred as heat to the chamber walls.

Since we are more concerned with producing a safe rocket motor we decided to utilize both regenerative and film cooling to ensure that the engine casing does not burn through. AUSROC II uses the total fuel flowrate, through a helical coil, for regenerative cooling. A ring of fuel injection holes will be located immediately upstream of the nozzle throat to reduce the transfer of heat in this critical region. Another ring of fuel injection holes, on the injector face, provides a cooling gas film layer adjacent to the chamber walls.

The amount of heat transferred by conduction from the chamber gas to the walls in a rocket thrust chamber is negligible. A part of the transferred heat is attributable to radiation. At low temperatures, radiation accounts for only a negligible portion of the total heat transferred and can usually be neglected. The absorption of radiation follows the same laws as those of emission. However, a highly reflective surface on the inside wall of the chamber tends to reduce absorption and to minimize the temperature increase of the walls. We decided to chrome plate the chamber wall to reduce the amount of radiated heat and thus, for simplicity, we neglected radiation in our calculations. By far the largest part of the heat is transferred by means of convection. For constant chamber pressure, the chamber wall surface area increases less rapidly than the volume as the thrust level is raised. Thus the cooling of chambers is generally easier in large engines. Therefore the capacity of the wall material or the coolant to absorb all the heat rejected by the hot gas is generally more critical in smaller size chambers.

The problem is basically one of heat and mass transport associated with conduction through a wall. It is shown schematically in Fig. 3.6. In calculating the heat transfer for the combustion chamber, the following process is undertaken:

#### **Conductive Heat Transfer:**

$$q = Q/A = -k \cdot A \cdot dT/dx$$

where:  $q$  = heat flux ( $W/m^2$ )  
 $Q$  = heat transfer rate (W)  
 $A$  = chamber surface area ( $m^2$ )  
 $k$  = thermal conductivity of chamber wall ( $W/m K$ )  
 $dT$  = temperature drop across chamber wall (K)  
 $dx$  = chamber wall thickness (m)

#### **Convective Heat Transfer:**

$$q = Q/A = h \cdot A \cdot dT$$

where:  $h$  = heat transfer coefficient ( $W/m^2 K$ )  
 $A$  = chamber surface area ( $m^2$ )

Therefore:

$$q = Q/A = h_g(T_g - T_{wg}) = k.(T_{wg} - T_{wl})/dx = h_l(T_{wl} - T_l)$$

$$q = (T_g - T_l) / ( 1/h_g + dx/k + 1/h_l )$$

The various coefficients used are determined as follows:

$$h_g = 0.026 (k/D) (Re) (Pr)$$

$$h_l = 0.023 (C_p m/A) (Re) (Pr)$$

Due to insufficient data, especially conductivity data for kerosene as a liquid and vapour at varying temperatures, we were unable to use the above formulae. An approximate value for  $h_l$  was found using the following empirical relation:

$$h_l = 0.002 C_p v \rho$$

where:  $C_p = 2090 \text{ J/kg K}$  (specific heat, Kero)  
 $v = 9 \text{ m/s}$  (coolant velocity, Kero)  
 $\rho = 580 \text{ kg/m}^3$  (density, Kero)

$$h_l = 21,820 \text{ W/m}^2 \text{ K}$$

Since we could not theoretically determine a value for  $h_g$ , we decided to assume a heat transfer rate and work backwards through the calculations to obtain the necessary temperatures. We decided to assume that 3% of the total energy generated in the combustion chamber is transferred, as heat, to the walls. This particular value is typical for chambers of this size.

$$\text{Total Heat Generated in Chamber} = 24.668 \text{ MW}$$

$$\text{Heat Transferred across Walls} = 24.668 \times 0.03 = 740,000 \text{ W}$$

$$\text{The Chamber surface area is calculated to be} = 0.1914 \text{ sq.m}$$

We can now calculate the various wall and liquid temperature as follows:

$$Q = h_g A (T_g - T_{wg}) = k A (T_{wg} - T_{wl})/dx \\ = h_l A dT = m C_p (T_{out} - T_{in})$$

where:  $T_{in} = 298 \text{ K}$  (Coolant entry temperature)  
 $T_{out} =$  Coolant exit temperature  
 $T_g = 3392 \text{ K}$  (combustion temperature)  
 $k = 35 \text{ W/m K}$  (mild steel at 600 C)  
 $dx = 0.003 \text{ m}$  (chamber wall thickness)

$$740,000 = 21,820 \times 0.1914 \times dT = 1.49 \times 2090 \times (T_{out} - 298)$$

Therefore:  $T_{out} = 536 \text{ K (263 C)}$

$$740,000 = 21,820 \times 0.1914 \times \frac{[(T_{wl} - T_{in}) - (T_{wl} - T_{out})]}{[\ln(T_{wl} - T_{in}) / (T_{wl} - T_{out})]}$$

(This theory implies constant chamber wall temperature)

Iterating gives:  $T_{wl} = 620 \text{ K (347 C)}$

$$740,000 = (35 \times 0.1914 \times (T_{wg} - T_{wl})) / 0.003$$

Hence:  $T_{wg} = 951 \text{ K (678 C)}$

$$740,000 = h_g \times 0.1914 \times (T_g - T_{wg})$$

Therefore:  $h_g = 1584 \text{ W/m}^2 \text{ K}$

The outer chamber wall temperatures can now be calculated as follows:

$$q = (T_1 - T_a) / (1/h_l + dx/k + 1/h_a)$$

where:  $T_1 = (298 + 536) / 2 = 417 \text{ K} = \text{mean liquid temperature}$   
 $T_a = 298 \text{ K} = \text{atmospheric temperature}$   
 $h_l = 21,820 \text{ W/m}^2 \text{ K}$   
 $dx = 0.002 \text{ m} = \text{outer wall thickness}$   
 $k = 52 \text{ W/m K (360 K)} = \text{conductivity of wall material}$   
 $h_a = 8 \text{ W/m}^2 \text{ K} = \text{atmospheric heat transfer coeff.}$

Therefore:  $q = 951 \text{ W/m}^2$

$$q = h_l \times (T_1 - T_{sl})$$

Thus:  $T_{sl} = 417 \text{ K (approx.)}$

$$q = k (T_{sl} - T_{sa}) / dx$$

Hence:  $T_{sa} = 417 \text{ K (approx.)}$

$$q = h_a (T_{sa} - T_a) = 8 \times (417 - 298) = 952 \text{ W/m}^2$$

This demonstrated that the free convection to the surrounding atmosphere is, by far, the most dominant component of heat transfer through the outer chamber wall.

### 3.3 HYDRAULIC LOSSES IN COOLING PASSAGE

The cooling coil or cooling jacket should be designed so that the fluid absorbs all the heat transferred across the inner wall, and so that the coolant pressure drop will be small. The high liquid coolant velocities necessary for good cooling unfortunately contribute to high pressure losses, which in turn necessitate a more powerful and heavier feed system. A typical pressure loss of a cooling jacket is between 5-25% of the chamber pressure. It is calculated as follows:

$$P_{\text{loss}} = f (L/D) ( \rho v_{\text{av}}^2 / 2 )$$

where:  $P_{\text{loss}}$  = pressure drop through cooling coil (Pa)  
 $f$  = friction factor  
 $L$  = cooling coil length (m)  
 $D$  = Hydraulic radius (m)  
 $v$  = mean coolant velocity (m/s)  
 $\rho$  = mean coolant density (kg/m<sup>3</sup>)  
 $m = \rho \times A_p \times v$

where:  $m = 1.49 \text{ kg/s}$  = mass flow of coolant  
 $\rho = 580 \text{ kg/m}^3$  = kerosene density (417 K)  
 $A_p = \text{passage area} = (0.008 \times 0.045) = 0.00036 \text{ m}^2$

Therefore:  $v = 7 \text{ m/s}$  (around chamber)

Since the greatest heat transfer rate occurs at the throat, it is necessary to increase the coolant velocity in this region. We decided to double the coolant velocity around the throat by halving the coolant passage area.

Thus:  $v = 14 \text{ m/s}$  (around throat)  
 $v_{\text{av}} = 9 \text{ m/s}$

The length of the coolant passage was measured to be 4.45 m. The hydraulic diameter for the mean passage area is obtained using:

$$D = 4 A_m / P_w$$

where:  $A_m = (0.04 \times 0.008) = 0.00032 \text{ m}^2$   
 $P_w = \text{Wetted Perimeter} = (2 \times 0.04 + 2 \times 0.008) = 0.096 \text{ m}$

Therefore:  $D = 0.0133 \text{ m}$

To calculate a value for  $f$ , we must use Reynolds # and the passage relative roughness.



$$\begin{aligned} \mathbf{Re} &= ( v D / \nu ) \quad \text{where: } \nu = \text{kinematic viscosity (m}^3\text{/s)} \\ &= ( 9 \times 0.0133 / 1.45\text{e-}06 ) = 82,552 \end{aligned}$$

Relative roughness ( $\lambda$ ) for commercial steel tube =  $4.5\text{e-}5$

$$\lambda / D = 0.00338$$

Using the Moody diagram we obtain a friction factor of:

$$f = 0.028$$

Solving for Ploss we get:

$$\begin{aligned} \mathbf{P_{loss}} &= 0.028 \times ( 4.45/0.0133 ) \times ( 580 \times 9^2 / 2 ) \\ &= 220,064 \text{ Pa ( 32 psi )} \end{aligned}$$

The helical coil which is wrapped around the inner chamber wall forms the coolant passage and is manufactured by tack welding a steel rod, with correct spacing, around the inner chamber wall.

### 3.4 CHAMBER MATERIAL AND STRESS ANALYSIS

We based the selection of the chamber wall material on the following parameters:

- 1/ Availability
- 2/ Cost
- 3/ Workability
- 4/ Heat conductivity
- 5/ Strength at high temperatures

**Table 3.1** shows the properties of some common combustion chamber materials. After an analysis of the various types of materials we found carbon steel (0.5%) to be most appropriate. Table 3.2 shows the various properties of the carbon steel which we chose to use for the combustion chamber.

The walls of all liquid propellant rocket thrust chambers are subject to radial and axial pressure loads, the reaction forces of the mounting device, acceleration loads, vibration loads and thermal expansion stresses. These loads are different for each rocket motor design and each motor unit has to be considered individually in determining wall strengths. Fig. 3.7 shows the pressure distribution through the cooling passage and combustion chamber for our engine. From this we can see that the greatest pressure differential, across the inner wall, occurs at the nozzle exit. Similarly, the greatest pressure differential across the outer wall occurs at the same location and is larger in magnitude.

**TABLE 3.2****PROPERTIES OF 0.5% CARBON STEEL ( GRADE A106 )**

Ultimate Tensile Strength:	302 K	430 MPa
	755	314
	811	252
	922	138
	977	93
	1033	62
Yield Strength:	302 K	290 MPa
	755	162
	811	139
	977	51
	1033	26
	Modulus of Elasticity:	294 K
477		168,921
589		148,237
700		127,553
811		106,868
922		86,184
Thermal conductivity:	273 K	55 W/m K
	373	52
	473	48
	573	45
	673	42
	873	35
	1073	31
	1273	29
Coefficient of thermal expansion:	293-373 K	3.61e-06 m/m K
	293-473	3.72e-06
	293-573	3.94e-06
	293-773	4.27e-06
	293-873	4.44e-06
	293-973	4.55e-06

Due to the regenerative coolant passage, the inner chamber wall is always subject to compressive pressure stresses while the outer wall is always subject to tensile pressure stresses. The temperature differential introduces a compressive stress on the inside and a tensile stress on the outside of the inner wall. The temperature stress ( $s$ ) can be calculated for cylindrical chamber walls which are thin in relation to their radius as follows:

$$s = 2 \lambda E (T_{wg} - T_{wl}) / (1 - \nu)$$

where:  $\lambda = 4.44e-06 \text{ m/m K} = \text{Coefficient of thermal expansion}$   
 $E = 107,000 \text{ Mpa} = \text{Modulus of Elasticity}$   
 $T_{wg} = 951 \text{ K}$   
 $T_{wl} = 620 \text{ K}$   
 $\nu = 0.3 = \text{Poisson's Ratio}$

Thus:  $s = 449 \text{ MPa}$

This value is considerably higher than yield strength for carbon steel which is around 150 MPa at 786 K. Temperature stresses frequently exceed the yield point. The materials experience a change in the yield strength and the modulus of elasticity with temperature. The above equation is only applicable to elastic deformations. The yielding of rocket thrust chamber wall material can be observed by the small and gradual contraction of the throat diameter.

The thickness of the inner chamber wall is obtained in conformance with the stress value ( $s$ ). For a cylinder under radial pressure:

$$s = dP r / t$$

where:  $dP = \text{pressure differential}$   
 $r = \text{chamber radius}$   
 $t = \text{chamber wall thickness}$

The worst stress condition occurs when the thrust chamber is restarted while the inner wall is still hot. This is the situation just prior to combustion starting, so the chamber pressure = 1 atm. and the coolant coil pressure is at its maximum.

$$\begin{aligned} \text{Max coil pressure} &= P_c + \text{Injector pressure drop} + P_{\text{loss}} \\ &= 2,000,000 + 500,000 + 220,064 \\ &= 2,720,064 \text{ Pa} \end{aligned}$$

The mean inner wall temperature =  $(951+620)/2 = 786 \text{ K}$

The yield strength of carbon steel at 786 K = 150 MPa

Thus:  $150,000,000 = 2,720,064 \times 0.077 / t$

Therefore:  $t = 1.4 \text{ mm}$

We decided to use an inner wall thickness of  $t = 3\text{mm}$ . This gives us a factor of safety (F.O.S.), for the worst case, of:

$$\text{F.O.S.} = 150,000,000 / 69,814,976 = 2.15$$

For the outer coolant passage wall, the worst case situation occurs when the wall temperature reaches a steady state value of 417 K with a passage pressure of 2,720,064 Pa. We decided to use a 2mm wall thickness for this application.

The yield strength of carbon steel at 417 K = 258 MPa

$$\text{F.O.S.} = 258,000,000 / 119,682,816 = 2.15$$

**Fig. 3.8** shows a typical stress distribution across a regeneratively cooled combustion chamber wall, and the overall effect of yielding due, primarily, to the temperature stresses. **Fig. 3.9** schematically shows the final chamber geometry.

### 3.5 ENGINE THRUST MOUNT

An engine thrust mount is used to connect the rocket motor to the rocket airframe. This mount must transfer the thrust load, produced by the engine, to the rest of the vehicle. It must also align the engine along the axis of the vehicle to eliminate overturning moments generated through thrust vector misalignment. Thus the thrust mount must be a strong and accurately manufactured item. With our rocket, we will be transferring the thrust load to rocket wall and, from there, along the length of the vehicle. We decided to flange mount the engine and injector to the thrust mount, through 12x10mm bolts, and attach the thrust mount to the rocket body via 20x8mm bolts. Aluminium was chosen for the thrust mount material due to its relatively high strength to weight ratio. **Fig 3.10** shows the design of the engine thrust mount.

## CHAPTER 4

### INJECTOR DESIGN

#### 4.1 INJECTOR DESIGN CALCULATIONS

The functions of the injector are similar to those of a carburettor in an internal combustion engine. The injector has to introduce and meter the flow to the combustion chamber, and atomize and mix the propellants in such a manner that a correctly proportioned, homogeneous fuel-oxidizer mixture will result, one that can readily be vapourized and burned. **Fig 4.1** shows several different types of injectors that are used in rocket propulsion. These various injector types are:

**1/ Impinging-Stream-Type Multiple-Hole Injectors** require the propellants to be injected through a number of separate small holes in such a manner that the fuel and oxidizer streams impinge on one another. Impingement aids atomization of the liquids into droplets and also aids distribution.

**2/ Nonimpinging or Shower Head Injectors** employ nonimpinging streams of propellant usually emerging normal to the face of the injector. It relies on turbulence and diffusion to achieve mixing.

**3/ Splash-Plate-Type Injectors** are intended to promote propellant mixing in the liquid state and use the principle of impinging the propellant streams against a surface.

**4/ Sheet or Spray-Type Injectors** give cylindrical, conical or other types of spray sheets. These sprays generally intersect and thereby promote mixing.

**5/ Premixing Injectors** require the mixing of liquid propellants before they are introduced into the combustion chamber.

We chose to use an impinging-stream-type, multiple-hole injector design incorporating 2 fuel streams and 1 oxidizer stream impinging on one another to produce a resulting flow pattern in the axial direction as shown in **Fig 4.2**. There will be 40 of these triplet injectors spaced evenly around the injector face.

The next step involves calculating the volumetric propellant flow rates:

$$dm/dt = F / v_c$$

where:  $m$  = propellant mass flow rate (kg/s)  
 $F = 9810 \text{ N}$  = rocket motor thrust  
 $v_c = (2450.3 \times 0.94) = 2303.3 \text{ m/s}$  = corrected velocity

$$dm/dt = 4.259 \text{ kg/s}$$

Our propellant mass ratio was determined from the thermochemical analysis to be 2.2. Thus we can calculate the mass flow rates of the fuel and oxidizer to be:

$$m_{\text{OX}} = 4.259 \times 2.2 / 3.2 = 2.928 \text{ kg/s}$$

$$m_{\text{f}} = 4.259 \times 1.0 / 3.2 = 1.331 \text{ kg/s}$$

Using the propellant densities we can obtain volumetric flow rates as follows:

$$\text{Density LOX} = 1141.1 \text{ kg/m}^3 \text{ (90 K)}$$

$$\text{Density JA-1} = 580 \text{ kg/m}^3 \text{ (536 K)}$$

$$V_{\text{OX}} = 2.928 / 1141.1 = 2.566 \text{ lt/s}$$

$$V_{\text{f}} = 1.331 / 580 = 2.295 \text{ lt/s}$$

The film cooling utilizes extra fuel and thus must be added to the above flow rate. We decided to inject 9.6% of the fuel flow rate as film cooling fluid at the injector face. The total fuel flow into the injector is now given as:

$$m_{\text{f}} = 1.331 \times 1.096 = 1.459 \text{ kg/s}$$

$$V_{\text{f}} = 2.295 \times 1.096 = 2.515 \text{ lt/s}$$

We set the rocket burn time to 20 sec thus the total propellant weights and volumes are given by:

$$m_{\text{f}} = 1.459 \times 20 = 29.2 \text{ kg}$$

$$V_{\text{f}} = 29.2 / 800 = 36.5 \text{ lt (298 K)}$$

$$m_{\text{OX}} = 2.928 \times 20 = 58.56 \text{ kg}$$

$$V_{\text{OX}} = 58.56 / 1141.1 = 51.319 \text{ lt}$$

The injection hole areas can be worked out using the following equation:

$$Q = C_d A v(2 dP/\rho)$$

Where:

- Q = volumetric flow rate (m<sup>3</sup>/s)
- C<sub>d</sub> = dimensionless discharge coefficient
- A = injection hole area (m<sup>2</sup>)
- ρ = injection density (kg/m<sup>3</sup>)
- dP = injector pressure drop (Pa)



The value of the discharge coefficient depends on the geometry of the injector passages. **Fig 4.3** shows the discharge coefficients for several different types of injectors. Our injector passages will closely resemble the short tube with rounded entrance type. The injector pressure drop was set at 500,000 Pa which should ensure good impingement and mixing of the propellants.

The LOX holes will have a  $C_d = 0.9$

The Kero holes will have a  $C_d = 0.88$

For LOX:  $0.002566 = 0.9 \times A_{OX} \sqrt{(2 \times 500,000 / 1141.1)}$

$$A_{OX} = 9.63e-05 \text{ m}^2$$

There are 40 LOX injectors, thus each injector has an area of:

$$A = 2.41e-06 \text{ m}^2$$

**LOX injector hole diameter = 1.75 mm**

For the combustible Kero flow:

$$0.002295 = 0.88 \times A_f \sqrt{(2 \times 500,000 / 580)}$$

$$A_f = 6.281e-05 \text{ m}^2$$

There are 80 Kero injectors, thus each injector has an area of:

$$A = 7.85e-07 \text{ m}^2$$

**Kero injector hole diameter = 1.00 mm**

The film cooling injection ring has a volumetric flow rate of:

$$2.295 \times 0.096 = 0.22 \text{ lt/s}$$

Thus, for the injector film cooling hole diameters:

$$0.00022 = 0.85 \times A \sqrt{(2 \times 500,000 / 580)}$$

$$A = 6.26e-06 \text{ m}^2$$

There are 32 film cooling holes on the injector face, therefore each hole has an area of:

$$A = 1.955e-07 \text{ m}^2$$

**Injector film cooling hole diameter = 0.5 mm**

## 4.2 INJECTOR MATERIAL AND GEOMETRY

The determination of the injector material posed some unique problems. The primary problem was one of heat transfer. The injector face would be absorbing heat from the combustion process as well as giving heat up to the propellants as they flow through the many manifolds and injection orifices. A relatively cool gas layer will form between the injector face and the main combustion zone as a result of the mixing and vapourization of propellants that occurs just downstream of the injector face. Thus the temperature of the injector face will never approach the combustion temperature.

Liquid oxygen enters the injector manifold and injection orifices at 90 K and acts as a coolant, absorbing the heat build up within the injector material. The Kerosene also acts as an injector coolant, though to a lesser extent than the LOX.

A further complication arises from the fact that 140 small injection holes must be drilled into the injector face. This produces manufacturing problems. A soft material would greatly assist in the manufacture of the injector.

With these situations in mind, it was necessary to use a material with a high thermal conductivity and easy workability. Two materials came to mind: copper and aluminium. Copper has the highest conductivity of any metal but also has a high density. Aluminium, on the other hand, has a high conductivity and a low density. Thus, aluminium (Grade 5083 H321) was chosen for the injector material. Aluminium melts at around 930 K but, with the gas film and coolant effects of the propellants, the temperature of the material should never reach this value. Due to the complexities involved, an exact temperature distribution across the injector could not be obtained. Accurate results for this problem must be obtained experimentally during a test firing.

The final injector configuration, including the positions of each injector orifice, manifold, seal and propellant line connection were determined geometrically on a CAD package. The final design utilizes O-ring seals and a flange mount. The Kerosene coolant bleeds directly into the injector fuel manifold from the helical coolant passage around the chamber through 16 5mm diameter holes.

**Figs. 4.4-4.6** show the final injector configuration and dimensions.

## CHAPTER 5

### DESIGN OF PROPELLANT STORAGE TANKS

#### 5.1 DETERMINATION OF TANK CONFIGURATION

A pressure feed bi-propellant liquid fuelled rocket consists of 2 propellant tanks, one for the fuel (Kerosene) and one for the oxidizer (LOX). There is also a high pressure gas supply tank which is used to maintain constant pressure in the propellant tanks. Tanks can be arranged in a variety of ways and the tank design can be used to exercise some control over the change in the location of the centre of gravity. Fig 5.1 shows some typical propellant tank arrangements. Because a propellant tank has to fly, its weight is at a premium and the tank material is, therefore, highly stressed. The stresses effecting the propellant tanks include:

- Internal Pressure Stresses
- Thrust Load Stresses
- Vibration Stresses
- Aerodynamic Stresses
- Temperature Stresses

Cryogenic propellants, such as Liquid Oxygen (90 K), cool the tank wall temperature far below the ambient air temperature. This causes condensation of moisture on the outside of the tank and usually the formation of ice prior to launch. The ice is undesirable since it increases the vehicle's inert weight and can cause problems with the successful operation of propellant valves. It is, therefore, necessary to insulate all tanks and propellant lines that carry cryogenic propellants. Cryogenic tanks must also be equipped with pressure relief vent valves since, even with good insulation, propellant boil-off is inevitable and must be catered for.

The optimum shape for a propellant tank is spherical, for it gives a tank with the least weight. Unfortunately, spheres are not very desirable shapes for large, main propellant tanks flying in the atmosphere. The propellant tanks are generally an integral part of the rocket airframe and usually conform to a cylindrical configuration.

In pressure feed rockets, the propellant tank pressure generally falls between 2-5 MPa (300-700 psi) while the pneumatic gas supply tank pressure falls between 7-35 MPa (1000-5000 psi). In rockets utilizing turbopumps, the propellant tanks need not hold any high pressure, thus their tank pressure usually falls between 0.07-0.35 MPa (10-50 psi). It is, therefore, apparent that in large rockets with big propellant storage tanks, turbopump vehicles will have a weight advantage over pressure feed vehicles.

We chose to use cylindrical propellant tanks with welded hemispherical end caps for our rocket. With the aim of reducing weight, it was also decided to make the walls of the tanks, the airframe of the vehicle. This eliminates the need for a separate airframe and mounting provisions. The tanks could not share a common bulkhead as the LOX would, undoubtedly, freeze the kerosene. Thus the tanks had to be separated by an intertank support. LOX has a higher specific gravity than kerosene, so we located the LOX tank above the kerosene tank in such a manner as to obtain a higher centre of gravity, and thus, giving the vehicle a higher natural aerodynamic stability. Since we decided not to use a separate airframe shell it was undesirable to pipe the LOX around the kerosene tank, as this would have created unnecessary drag. We decided, instead, to pipe the LOX through the centre of the kerosene tank, directly to the top of the main LOX valve.

This was done by welding a pipe through the centre of the kerosene tank and allowing a second insulated pipe, carrying the LOX, to pass through it. The inner tank diameter was set at 250mm and the tank lengths were determined as follows:

$$V_{ox} = 51.32 \text{ lt (allow for some boil-off)} = 54 \text{ lt}$$

$$V_f = 36.50 \text{ lt (allow slight excess)} = 39 \text{ lt}$$

$$\text{Tank radius} = 0.25 / 2 = 0.125\text{m}$$

For the LOX tank:  $V_{ox} = (\pi r^2 L) + (4/3 \pi r^3)$

$$L = 0.95 \text{ m (cylinder length)}$$

The kero tank has a 60mm OD pipe through the centre of it so this must be subtracted from the total volume.

For the kerosene tank:  $V_f = (\pi r^2 L) + (4/3 \pi r^3) - (\pi 0.03^2)(L + 0.25)$

$$L = 0.69 \text{ m (cylinder length)}$$

## 5.2 TANK MATERIAL SELECTION & STRESS ANALYSIS

The materials most suitable for use as propellant tanks for Liquid oxygen and Kerosene are, primarily, Stainless Steels and Aluminium alloys. Of these 2, the aluminium alloys have the highest strength to weight ratio and were, therefore, chosen to be used for our tank material. Table 5.1 shows the properties of aluminium alloy, grade 5083 in annealed and work hardened (H321) states.

The propellant tank pressure stress ( $\sigma_t$ ) can be worked out as follows:

$$\sigma_t = P \times r / t$$

The individual tank pressures are obtained as:

$$\begin{aligned} P_{(\text{kero tank})} &= P_{\text{chamber}} + P_{\text{coil}} + P_{\text{injector}} \\ &= 2,000,000 + 220,064 + 500,000 \\ &= 2,720,064 \text{ Pa} \end{aligned}$$

$$\begin{aligned} P_{(\text{Lox tank})} &= P_{\text{chamber}} + P_{\text{injector}} \\ &= 2,000,000 + 500,000 \\ &= 2,500,000 \text{ Pa} \end{aligned}$$

For a 4mm tank wall thickness we get:

$$\begin{aligned} \text{Kerosene tank stress} &= 2,720,064 \times 0.125 / 0.004 \\ &= 85 \text{ MPa} \end{aligned}$$

Minimum welded yield strength = 165 MPa

$$\text{Therefore: F.O.S.} = 165 / 85 = 1.94$$

$$\begin{aligned} \text{LOX tank stress} &= 2,500,000 \times 0.125 / 0.004 \\ &= 78 \text{ MPa} \end{aligned}$$

Minimum welded yield strength (80 K) = 165

$$\text{Therefore, F.O.S.} = 165 / 78 = 2.12$$

**Fig 5.2** shows the LOX tank configuration and **Fig 5.3** shows the kerosene tank configuration.

**TABLE 5.1****PROPERTIES OF 5083 ALUMINIUM ALLOY**

PROPERTY	Temp	0 TEMPER	H321 (Work Hardened)
$\sigma_T$ (min,MPa)	80K	407	
	298K	290	300
	640K	41	
$\sigma_Y$ (min,MPa)	80K	165	
	298K	145	213
	640K	29	
$\sigma_Y$ Welded (min,MPa)	80K	165	
	298K	145	165
	640K	29	
Elongation (%)	80K	36	
	298K	25	10
	640K	130	
Elastic Modulus (MPa)	298K	71,000	71,000
Hardness (Birnell)	298K	67	82
Coeff. Thermal Exp.	298K	$23.76 \times 10^{-6}$	$23.76 \times 10^{-6}$
Density (kg/m <sup>3</sup> )	298K	2658	2658
Corrosion Resistance		good	good
Weldability		good	good
Machinability		good	good

## CHAPTER 6

### DESIGN OF PRESSURE FEED SYSTEM

#### 6.1 PRESSURE FEED REQUIREMENTS

The simplest means of pressurizing the propellants is to force them out of their respective tanks by displacing them with high pressure gas. This gas is fed into the propellant tanks at a controlled pressure, thereby giving a controlled propellant discharge. For AUSROC II, a gas pressure feed system will be light weight when compared with an equivalent turbopump system. A simple pressurized feed system is shown schematically in Fig. 1.2. It consists essentially of a high pressure gas tank, a gas shut-off and starting valve, a pressure regulator, propellant tanks, propellant valves, and feed lines. Addition components, such as filling and draining provisions, check valves, vent valves and filters, are also often incorporated.

After all tanks are filled, the high pressure gas valve is remotely actuated and admits gas through the pressure regulators at a constant pressure to the propellant tanks. The propellants are then fed to the thrust chamber by opening the main propellant valves. When the propellants are completely consumed, the pressurizing gas serves, also, as a scavenging agent and cleans lines and valves of liquid propellant residue. The first part of gas leaving the high pressure storage tank is at, or slightly below ambient temperature. The gas remaining in the tank undergoes an isentropic expansion, causing the temperature of the gas to decrease steadily. The last portion of the pressurizing gas leaving the tank will be very much colder than the ambient temperature and will readily absorb heat from the piping and the tank walls. In our actual propulsion system installation, the pressurized gas is required to perform a secondary function of operating the system valves. In pressurizing LOX, some of the pressurizing gas is condensed or dissolved and, therefore, not fully effective as a pressurizing agent. A low-freezing inert gas, such as helium, is best suited for forcing LOX out of tanks.

In general, 2.5 times as much nitrogen weight is needed for pressurizing LOX, as compared to the nitrogen needed for displacing an equivalent volume of water at the same pressure. It is for this reason that we chose to use helium as the pressurizing gas for AUSROC II. Helium is more expensive and less available than nitrogen but its performance as a pressurizing gas is much better than that of nitrogen.

The quantity of pressurizing gas required for AUSROC II is determined as follows:

$$P V = n R T_a$$

where: P = Pressure (Pa)  
V = Volume (m<sup>3</sup>)  
n = Number of Mol  
R = 8.314 = Gas Constant  
T<sub>a</sub> = 298 K = Ambient Temp.

For LOX tank:  $n = 2,500,000 \times 0.054 / 8.314 \times 298$   
**n = 54.5 mol**

For Kerosene tank:  $n = 2,720,064 \times 0.039 / 8.314 \times 298$   
**n = 42.8 mol**

For Residual gas in bottle:  
 $n = 2,720,064 \times 0.016 / 8.314 \times 298$   
**n = 17.6 mol**

**Total = 42.8 + 54.5 + 17.6 = 114.9**

(Molecular weight of helium = 4 g/mol)

**m = n x Mr = 114.9 x 4 = 459.6 g (He)**

We will be using a commercially available gas bottle for our high pressure supply with the following specifications:

**Type:** Glass-Fibre reinforced alloy bottle  
**Water Volume:** 16 lt  
**Length:** 880 mm  
**Width:** 175 mm  
**Weight:** 11.5 kg  
**Test Pressure:** 34 MPa (4900 psi)

The helium bottle pressure that is required to deliver the necessary quantity of gas is found by:

$$P V = n R T_a$$

$$P = 114.9 \times 8.314 \times 298 / 0.016$$
$$= 17.792 \text{ MPa (2580 psi)}$$

Filling the bottle to 20 MPa would ensure ample gas supply and pressure differential for the successful operation of the regulators and for tank and line scavenging after burnout.



## 6.2 COMPONENT SELECTION FOR FEED SYSTEM

The types of valves used in propellant feed systems are various and can be classified as follows:

- 1/ **FLUID TYPE:** fuel, oxidizer, gas etc.
- 2/ **MODE OF ACTUATION:** pneumatic, hydraulic, solenoid etc.
- 3/ **APPLICATION OR USE:** propellant control, gas feed, etc.
- 4/ **VALVE TYPE:** ball, butterfly, plug, needle etc.

The valves in rockets have to be foolproof, since any leakage or valve failure can cause a failure of the rocket unit itself. All valves are tested for 2 qualities prior to installation; they are tested for leaks and for functional soundness. The propellant valves in rocket units handle relatively large flows at high service pressures. Therefore, the forces necessary to actuate the valves are large. Hydraulic or pneumatic pressure, controlled by pilot valves, operate the larger valves. These pilot valves are, in turn, actuated by a solenoid or mechanical linkage. This is essentially a means of power boost.

In AUSROC II we decided to use ball valves due to their high flow characteristics and relatively low weight. To actuate the ball valves we will be using pneumatic actuators since we have a readily available supply of pressurizing gas. These actuators will, in turn, be triggered by electrically operated solenoids. The LOX ball valve has special cryogenic seats, to allow operation at low temperatures. Due to flow constraints we will be using a 25mm ball valve for the LOX, a 20mm ball valve for the Kerosene, and a 10mm ball valve for the Helium. Each of these valves has its own pneumatic actuator and solenoid. There is a possibility that the LOX valve could freeze shut due to icing. To reduce the probability of this occurring we decided to wrap the LOX valve actuator stem with a 'Heat Trace' material powered by an external battery. This will reduce the ice build up but may also increase the LOX boil off rate slightly.

There will be 3 pressure regulators in operation within the rocket; 1 for each of the 2 propellant tanks and 1 for the pneumatic actuators. The pneumatic actuators will be operated at 700,000 Pa (100 psi) while the tank pressures will be as mentioned above. The gas flow rate into the tanks is quite large as shown below:

$$\begin{aligned} \text{LOX Tank,} \quad Q &= (54 \times 2,500,000) / (101,325 \times 20) \\ &= 66.62 \text{ std.lit/sec} \\ &= 142 \text{ std cubic ft. per minute (S.C.F.M)} \end{aligned}$$

$$\begin{aligned} \text{Kero Tank,} \quad Q &= (39 \times 2,720,064) / (101,325 \times 20) \\ &= 52.4 \text{ std.lit/sec} \\ &= 111 \text{ S.C.F.M.} \end{aligned}$$

Normal regulators do not handle flow rates of this size. After numerous searches (Australia wide) we found some compact light weight regulators with suitable flow characteristics. Further specifications on each of these valves and regulators can be found in **Appendix D**.

A plumbing layout for AUSROC II is shown in **Fig. 6.1**. Both LOX and Kerosene tanks will have venting provisions such that, in the result of a pressure surge or excess propellant boil-off, the tanks will not rupture. Check valves are not required in this particular design since the flow cannot pass back through the regulators. Fuelling ports with threaded sealing caps will be located on the top of the tanks in easy access locations. This will simplify the fuelling procedure on the launch rack. Due to the effects of thermal contraction at low temperatures and the associated stresses involved, it was decided to use a flexible, braided steel tube to carry the LOX from the LOX tank to the ball valve. In this manner, the contractions caused, in the LOX line, by the drop in temperature during fuelling, can be catered for.

## **CHAPTER 7**

### **PAYLOAD AND RECOVERY MODULES**

#### **7.1 PAYLOAD FACILITIES**

AUSROC II is not being designed as a freight carrying vehicle. Its primary goal is to undergo a series of test firings and analyses to relate the theoretical calculations to the practical situation. To do this we have to be able to sense various system parameters, analyse and process them and store the resulting data. It is the task of the telemetry system to perform these functions.

The data we wish to obtain from the dynamic firing of the vehicle include:

1. Combustion Chamber Pressure
2. Atmospheric Pressure
3. Accelerations
4. Velocities
5. Displacements
7. On-Board Video Footage

Some of this data is necessary to control the recovery system and must be processed on-board the vehicle.

AUSROC II will incorporate a tri-axial accelerometer. The values obtained from these 3 sensors will be mathematically manipulated to give the accelerations in all 3 axis. The combustion chamber pressure can be measured using a pressure transducer and the value used to assess the performance of the rocket motor. Atmospheric pressure is used to determine the correct height for deployment of the main parachute and will be discussed in more detail later.

An on-board video camera and video transmitter will send live video coverage from the vehicle to a ground receiver on UHF band (444 MHz) such that reception can be obtained using a UHF television set. The video sound channel will be used to transmit the data from the sensors to the ground for processing and storage. 1 Megabyte of onboard eprom storage will act as a backup storage medium for the data in the case of a transmission failure.

The electronics unit and microprocessor will also control the rocket startup procedure and recovery system. A major part of this project involved the integration of the electronics and rocket hardware into a compatible size and weight unit.

The electronics design work is being done through the Monash Uni. Electrical Engineering Department by Dominic Marinelli. He has undertaken this design work as his final year project thesis. The project thus required continuous interaction between Dominic and ourselves to maintain system compatibilities, and coordination throughout the development of this project. The electronics design and report will, therefore, form a supplement to this report at a later date.

## **7.2 RECOVERY SYSTEM**

One of the most important requirements of this project is to be able to recover the vehicle after it has been launched. Only after having recovered the rocket will we be able to perform an accurate analysis on its actual flight performance, and the physical state of the equipment after firing. The simplest means of recovery is through the use of a parachute. AUSROC II will reach an altitude in excess of 30km, and a speed greater than 2000 km/hr. For these reasons, it is essential to determine the correct time and position for deployment of the recovery system. It is the task of the telemetry system to determine this deployment scenario.

The optimum point for initial recovery system deployment for a ballistic flight path is at its peak altitude, since at this point the vehicle is travelling the slowest. This would result in the least stress imposed on the vehicle, due to parachute deployment. The INU senses angular displacements in each of the 3 axes. Thus, when either the pitch or yaw angular displacement exceeds 90 degrees, the parachute deployment system will be activated. The nose cone is to be ejected to allow the parachute to be deployed from the front of the rocket. This will be done through the use of a solenoid and two interconnected cable driven latches, which hold the nose cone to the vehicle. The nose is then pushed away from the body by a spring. When this occurs, the rocket experiences a sudden rotation from a nose-forward to a tail-forward position. This can cause large non-axial stresses on the rocket airframe, if the main parachute is deployed at this point. It is for this reason that smaller drogue parachutes are used. They are deployed at peak to stabilize the rocket, for easy main parachute deployment at a later time.

In AUSROC II we will be using a 1.5m drogue parachute, to be deployed at peak, to stabilize the rocket. The mount for the drogue will be firmly attached to the rocket body, such that the forces induced, at deployment, can be evenly distributed throughout the airframe. Fig. 7.1 shows the drogue mount attachment, and its position within the airframe.

When the atmospheric pressure sensor, within the telemetry system, registers a pressure equivalent to a height less than 3000m, a signal will trigger an explosive bolt to release the drogue parachute, and allow it

to pull out the main parachute. The main support arms for the drogue are pivoted outwards when the explosive bolt is fired, thus clearing the way for main parachute deployment. The main parachute mount is also rigidly attached to the airframe, to allow even distribution of the shock load imposed on it. The drogue slows the vehicle to a speed low enough to allow the main parachute to be deployed without inducing severely high stresses on the vehicle. **Fig. 7.1** further shows the main parachute mount and its position within the airframe.

There are many different types of parachute geometry. **Appendix G** shows the drag coefficients and other associated data for various parachute geometries. Both the drogue and main parachutes, used in AUSROC II, will be of a flat circular type, since these are readily available and easy to obtain.

Descent rates can be determined using the following equation:

$$F = m g = 0.5 C_d \rho A v^2$$

where:

- F = Drag Force (N)
- m = Rocket Dry Weight = 130 kg (approx.)
- g = Gravity = 9.81 m/s<sup>2</sup>
- C<sub>d</sub> = Drag Coefficient = 0.8
- ρ = Atmospheric Density (kg/m<sup>3</sup>)
- A = Parachute Cross-sectional Area (m<sup>2</sup>)
- v = Terminal Velocity (m/s)

For the drogue (area=1.77 m<sup>2</sup>), the descent rate will be calculated just prior to main parachute release, i.e. 3000m (ρ = 0.91 kg/cu.m):

$$130 \times 9.81 = 0.5 \times 0.8 \times 0.91 \times 1.77 \times v^2$$

Therefore:  $v = 44.5 \text{ m/s (160 km/hr)}$

For the main (area = 43 sq.m), the descent rate will be calculated at sea level, since this is where the rocket will hit the ground (ρ=1.22 kg/m<sup>3</sup>):

$$130 \times 9.81 = 0.5 \times 0.8 \times 1.22 \times 43 \times v^2$$

Therefore:  $v = 7.8 \text{ m/s (28 km/hr) = landing impact speed}$

The electronics, which are the most delicate components onboard the vehicle, will be protected from the impact, due to landing and dynamic system vibrations, by rubber shock mounts.

# CHAPTER 8

## LAUNCH INFRASTRUCTURE

### 8.1 LAUNCH RACK REQUIREMENTS

The major purpose of the launch rack is to provide guidance and stability for the vehicle, during its critical time of flight. Since there will be no active guidance onboard the rocket, the rack will stabilize the vehicle for the first 10m of its trajectory. At this time, the rocket will be travelling at approximately 100 km/hr. At this speed the fins will be able to supply the necessary stabilizing moment to keep the vehicle heading in the right direction.

Since rocket projectiles are essentially unguided missiles, the accuracy of following a required trajectory will depend on the initial aiming and the dispersion induced by uneven drag, wind forces, oscillations and misalignment of jet, body and fins. Deviations from the intended flight path are amplified if the projectile is moving at a low initial velocity, because the aerodynamic stability of a projectile with fins is small at low flight speeds.

For the launch rack to be practical, it must accommodate for different launch angles, easy vehicle loading and provisions for fuelling. The launch rack, however, must be able to be lowered to a horizontal position to allow the rocket to be mounted easily. The lowering and raising of the launch rail will be assisted by the use of a winch setup, thus minimizing physical effort. Once the launch rack has been raised to the required launch angle, there must be provisions to allow access to the propellant tanks which will be some distance above the ground level for fuelling. This access will be in the form of a ladder, where rungs protrude from the rear of the launch rack.

Finally, it is necessary to consider the ease of transportation and assembly of the launch rack. The cost involved in manufacturing the launch rack was also a necessary consideration. The rack, once disassembled, will be in the form of L-sections, T-sections and square tubing, with no single length being greater than 8m. This will allow minimal space for storage. Assembly of the rack will simply require the bolting of the various segments together.

## **8.2 ROCKET LAUNCH LUGS**

The mounting of the rocket onto the launch rack will be such that it hangs on the underside of the T-rail, as shown in **Fig 8.1**. Two launch lugs along one side of the rocket will be in the form of C-sections which readily slide along the T-rail. The lugs will be bolted to the side of the rocket. This will cause a slight increase in the rocket drag, on one side. Balance can be maintained by placing 2 identical launch lugs on the opposite side of the vehicle. Launch lugs which retract into the side of the rocket would be more ideal but they introduce other manufacturing and operation problems. **Fig. 8.2** shows the design of the rocket launch lugs.

## **8.3 STATIC TEST FACILITIES**

Another major function of the launch rack is to enable a static firing test to be performed on the completed rocket. This, of course, would require the rack to be pegged into the ground very firmly. The rocket will be bolted securely to the launch rack via the engine thrust mount. Strain gauges will then be positioned onto the launch rack to measure the force induced upon it by the rocket. This will, in fact, provide us with an indication of the thrust produced and how well it compares with our initial specification of 9810 N.

## **8.4 LAUNCH RACK CONFIGURATION**

In the assembled form, the launch rack essentially consists of a T-rail welded to a square section support, a winch mount and wire guide each mounted to a base frame, with extra supports for added strength. The T-rail has 2 main support arms and a tension wire to keep it in position. The winch has 2 side supports and one forward support to provide stability in all directions. The wire guide has 2 supports in a front-to-side direction. Its height, of more than twice the height of the winch, allows a moment to develop when the T-rail has been lowered to a horizontal level. The T-rail pivot point is 1m above the ground and has 2 rear supports for stability. The base frame has an overall dimension of 4x7m and will be firmly pegged into the ground. **Figs 8.3-8.5** shows the launch rack assembly in 3 different views.